Cancer Immunology, Immunotherapy (2025) 74:314
https://doi.org/10.1007/s00262-025-04182-1

RESEARCH

Spatially resolved endothelial signaling via nampt-itga5 drives immune evasion in stem-like gastric cancer

Ji-Yong Sung[1,2] · Jae-Ho Cheong[3] · Eui Tae Kim[4,5]

Received: 1 July 2025 / Accepted: 15 September 2025 / Published online: 29 September 2025

Abstract

Background Stem-like gastric cancer (GC) is an aggressive molecular subtype marked by poor prognosis and limited response to immune checkpoint blockade (ICB). The spatial mechanisms driving this resistance remain unclear.

Methods We conducted spatially resolved single-cell transcriptomic profiling of diffuse-type GC tissues to uncover the spatial architecture and functional diversity of tumor and stromal populations. Cellular heterogeneity and region-specific signaling pathways were characterized using integrative bioinformatics analyses.

Results We identified transcriptionally diverse, high-entropy cell populations predominantly localized in the deep tumor regions. These included unique endothelial and fibroblast subsets enriched for pro-tumorigenic and immune-regulatory signaling. A notable finding was the engagement of deep-region endothelial cells in *VISFATIN* (extracellular *NAMPT*) signaling through the *ITGA5–ITGB1* integrin axis, associated with immune evasion and poor prognosis. This endothelial signaling program is distinct from and functionally independent of cancer-associated fibroblast (CAF)-mediated pathways. Elevated expression of the *NAMPT–ITGA5–ITGB1* axis was observed in ICB non-responders and correlated with reduced overall survival.

Conclusions Our study delineates spatially defined cellular programs that contribute to immune escape in stem-like GC, highlighting a novel VISFATIN–integrin signaling axis as a potential biomarker and therapeutic target in immunotherapy-resistant tumors.

Keywords Stem-like gastric cancer · Endothelial cells · VISFATIN · NAMPT · Immune evasion · Immunotherapy resistance

✉ Ji-Yong Sung
5rangepineapple@gmail.com

✉ Jae-Ho Cheong
jhcheong@yuhs.ac

✉ Eui Tae Kim
tae@jejunu.ac.kr

[1] Department of Biological Sciences, College of Natural Sciences, Seoul National University, Seoul 08826, Republic of Korea

[2] Department of Neurosurgery, Seoul National University Bundang Hospital, Seoul National University College of Medicine, Seongnam-Si, Republic of Korea

[3] Department of Surgery, Yonsei University College of Medicine, Seoul 03722, Republic of Korea

[4] Department of Microbiology and Immunology, Jeju National University College of Medicine, Jeju 63241, Republic of Korea

[5] Jeju Research Center for Natural Medicine, Jeju National University Core Research Institute, Jeju, Republic of Korea

Introduction

Gastric cancer (GC) remains a significant global health burden, particularly in East Asia, due to its high incidence and mortality rates [1]. Among its molecular subtypes, the stem-like subtype is associated with the poorest prognosis and exhibits marked resistance to conventional therapies, including chemotherapy and immune checkpoint blockade (ICB) [2–4]. Despite its clinical relevance, therapeutic strategies targeting this subtype are lacking, and its underlying biology remains incompletely understood.

Recent studies have highlighted the pivotal role of the tumor microenvironment (TME) in promoting stem-like phenotypes and therapeutic resistance. Cancer-associated fibroblasts (CAFs) and endothelial cells (ECs) are key stromal components that contribute to these processes through paracrine signaling, immune suppression, and extracellular matrix remodeling [5, 6]. The stem-like subtype has been

shown to possess a unique telomere maintenance mechanism (TMM) [7], and CAFs significantly contribute to tumor evolution and immune evasion [2] [8] [9]. Furthermore, stem-like tumors exhibit heterogeneity in Naba core matrisome composition [10] and undergo extensive metabolic reprogramming, including shifts in oxidative metabolism and fatty acid oxidation [11] [12]. Single-cell transcriptomic analyses have revealed that deep tumor regions in diffuse-type GC are enriched with high-entropy stromal and epithelial cell populations, exhibiting elevated activity of pathways such as *VEGFA–VEGFR2*, Hedgehog, and Hippo-YAP [13, 14].

In the context of intercellular communication within the TME, the nicotinamide phosphoribosyltransferase (NAMPT) signaling pathway has been implicated in tumor progression and immune modulation. Studies in colorectal cancer have identified interactions between *NAMPT* and integrin receptors, specifically integrin subunit alpha 5 (*ITGA5*) and integrin subunit beta 1 (*ITGB1*), suggesting a role in stromal remodeling and tumor progression [15, 16]. While these studies focused on fibroblast contexts, the endothelial-specific role of the *NAMPT–ITGA5–ITGB1* axis in gastric cancer remains poorly defined.

In this study, we performed single-cell RNA sequencing (scRNA-seq) analyses of superficial and deep regions of diffuse-type GC to delineate the cellular and molecular drivers of stem-like evolution [17]. We identify a transcriptionally active subpopulation of *ITGA5*$^+$ endothelial cells enriched in the deep tumor microenvironment, which interact with fibroblasts and immune cells via the *NAMPT* axis. Our findings provide mechanistic insights into spatial tumor ecology and support the development of novel biomarker-driven strategies for overcoming treatment resistance in stem-like gastric cancer.

Methods

Bulk RNA-seq and single-cell RNA-seq data acquisition

We analyzed publicly available transcriptomic datasets and an institutional cohort to explore the molecular features of the stem-like subtype in gastric cancer. Bulk RNA-seq data were obtained from The Cancer Genome Atlas Stomach Adenocarcinoma (TCGA-STAD) project and the Y497 (Yonsei hospital cohort, GSE84433). Immune checkpoint blockade (ICB) response was predicted using the Tumor Immune Dysfunction and Exclusion (TIDE) algorithm (http://tide.dfci.harvard.edu). Single-cell data were downloaded from the Gene Expression Omnibus under accession number GSE167297, which includes five diffuse-type gastric cancer patients with spatial annotation of deep and superficial tumor regions. Raw count matrices were processed using Seurat v4.1.1 in R v4.2.1. Quality control included the exclusion of cells with fewer than 200 or more than 5,000 detected genes and cells with > 10% mitochondrial gene content. Genes expressed in fewer than three cells were removed. Data normalization, variable feature selection, and integration were performed using the standard Seurat workflow, followed by dimensionality reduction with principal component analysis and UMAP.

High-entropy cell identification and stemness assessment

To identify transcriptionally diverse cell populations, cell-wise Shannon entropy was calculated using the StemID algorithm [18]. Cells with entropy values in the top decile across the dataset were defined as high-entropy cells. These cells were stratified by cluster and anatomical region to assess spatial and cell type-specific entropy distributions. Gene Ontology (GO) enrichment analysis for high-entropy clusters was performed using Metascape [19], with default significance thresholds (adjusted $p < 0.01$, minimum enrichment > 1.5-fold).

Pathway enrichment and molecular subtype scoring

Cancer hallmark pathway activity was evaluated using Gene Set Variation Analysis (GSVA) with gene sets from MSigDB v7.5.1 [20]. GSVA was applied to normalized log-transformed expression data to compute enrichment scores for hallmark pathways. Pathways with GSVA scores exceeding 0.4 and adjusted p-values < 0.05 were considered biologically significant for downstream interpretation. Gastric cancer molecular subtype scoring was performed using previously defined signatures for the gastric, inflammatory, proliferative, metabolic, and stem-like subtypes [21–24]. Single-cell level enrichment was calculated using Seurat's AddModuleScore function, and cells with a module score > 0.2 z-score over the sample mean were considered subtype-enriched.

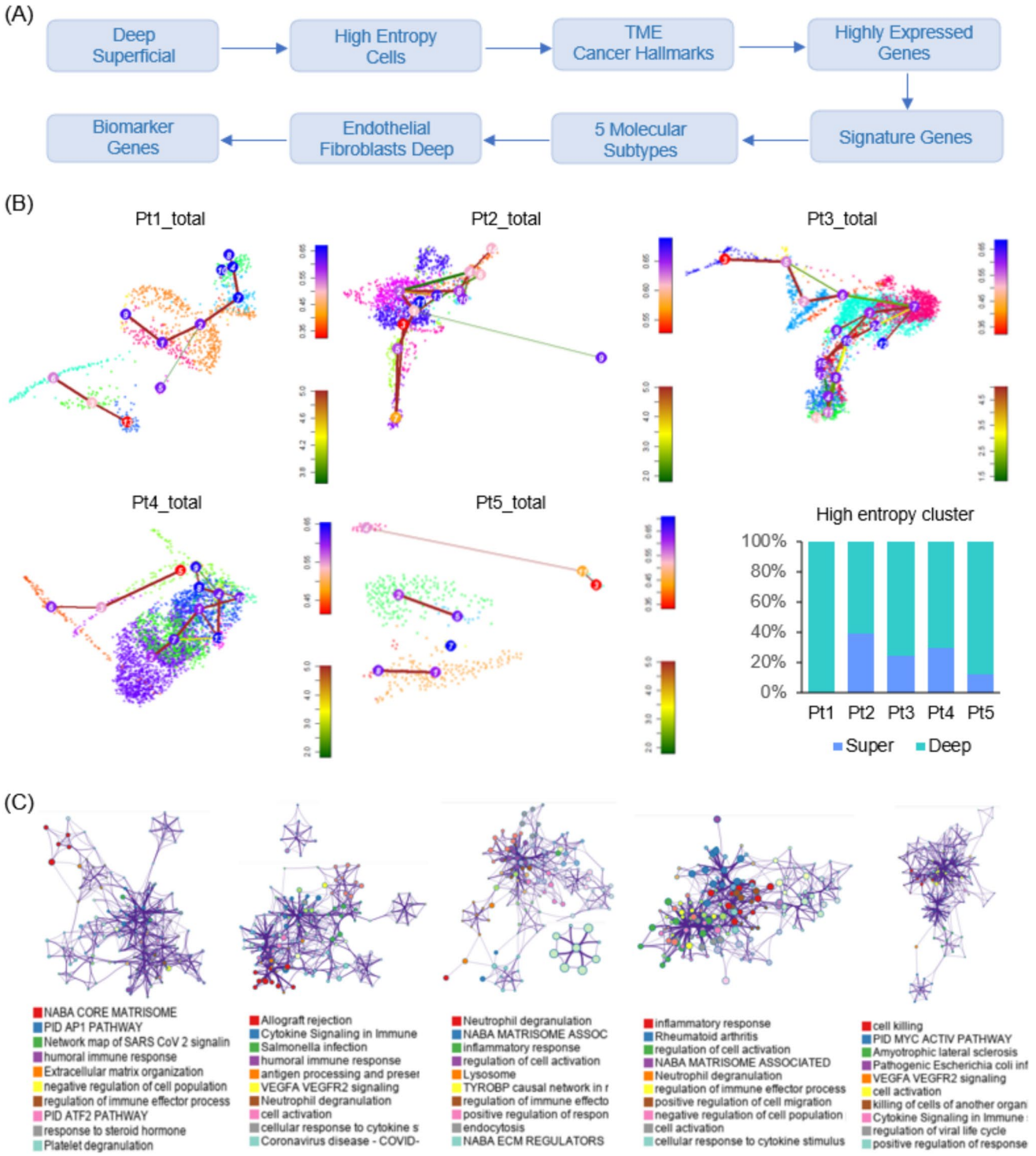

Fig. 1 High-entropy cells are enriched in deep regions of diffuse-type gastric cancer. **A** Schematic overview of the analysis pipeline. Tumor tissues from five patients were dissected into deep and superficial regions for single-cell RNA sequencing (scRNA-seq). High-entropy cells were identified using StemID and analyzed for tumor microenvironment (TME) features, cancer hallmark pathway activity, molecular subtype signatures, and biomarker expression. **B** t-SNE plots with pseudotime-based trajectory inference for each patient (Pt1–Pt5). High-entropy clusters (black circles) are predominantly located in the deep regions. Bar plots summarize the proportion of high-entropy cells per region, confirming a consistent deep-region bias. **C** Gene Ontology (GO) enrichment networks of high-entropy clusters. Common enriched pathways include extracellular matrix (ECM) remodeling (e.g., NABA*NABA* core matrisome), angiogenesis (e.g., *VEGFA/VEGFR2* signaling), immune regulation (e.g., cytokine and humoral responses), and stress response (e.g., apoptosis, hypoxia), reflecting spatial and inter-patient heterogeneity

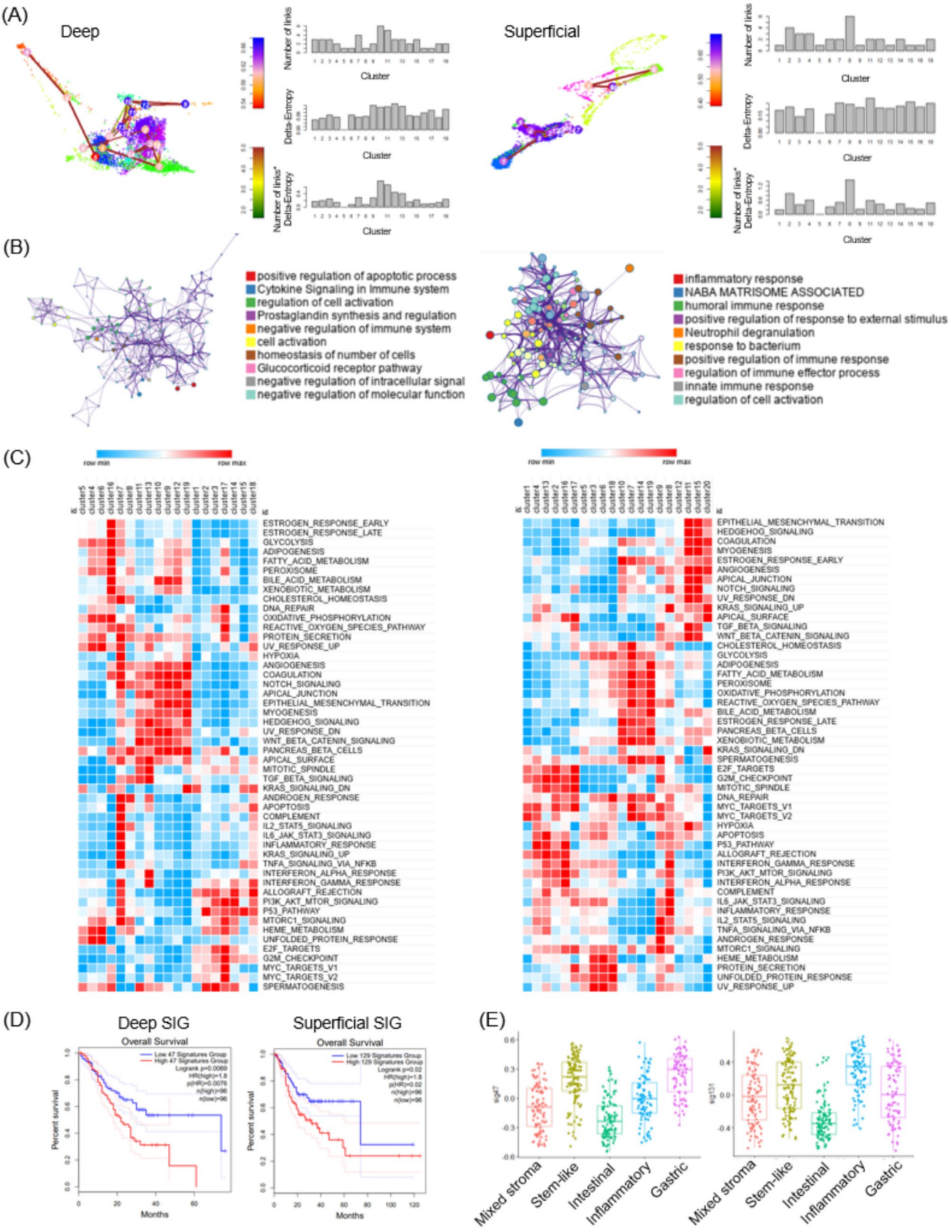
(A)
Deep
Superficial
Number of links
Delta-Entropy
Number of links*Delta-Entropy
Cluster
(B)
positive regulation of apoptotic process
Cytokine Signaling in Immune system
regulation of cell activation
Prostaglandin synthesis and regulation
negative regulation of immune system
cell activation
homeostasis of number of cells
Glucocorticoid receptor pathway
negative regulation of intracellular signal
negative regulation of molecular function
inflammatory response
NABA MATRISOME ASSOCIATED
humoral immune response
positive regulation of response to external stimulus
Neutrophil degranulation
response to bacterium
positive regulation of immune response
regulation of immune effector process
innate immune response
regulation of cell activation
(C)
row min
row max
ESTROGEN_RESPONSE_EARLY
ESTROGEN_RESPONSE_LATE
GLYCOLYSIS
ADIPOGENESIS
FATTY_ACID_METABOLISM
PEROXISOME
BILE_ACID_METABOLISM
XENOBIOTIC_METABOLISM
CHOLESTEROL_HOMEOSTASIS
DNA_REPAIR
OXIDATIVE_PHOSPHORYLATION
REACTIVE_OXYGEN_SPECIES_PATHWAY
PROTEIN_SECRETION
UV_RESPONSE_UP
HYPOXIA
ANGIOGENESIS
COAGULATION
NOTCH_SIGNALING
APICAL_JUNCTION
EPITHELIAL_MESENCHYMAL_TRANSITION
MYOGENESIS
HEDGEHOG_SIGNALING
UV_RESPONSE_DN
WNT_BETA_CATENIN_SIGNALING
PANCREAS_BETA_CELLS
APICAL_SURFACE
MITOTIC_SPINDLE
TGF_BETA_SIGNALING
KRAS_SIGNALING_DN
ANDROGEN_RESPONSE
APOPTOSIS
COMPLEMENT
IL2_STAT5_SIGNALING
IL6_JAK_STAT3_SIGNALING
INFLAMMATORY_RESPONSE
KRAS_SIGNALING_UP
TNFA_SIGNALING_VIA_NFKB
INTERFERON_ALPHA_RESPONSE
INTERFERON_GAMMA_RESPONSE
ALLOGRAFT_REJECTION
PI3K_AKT_MTOR_SIGNALING
P53_PATHWAY
MTORC1_SIGNALING
HEME_METABOLISM
UNFOLDED_PROTEIN_RESPONSE
E2F_TARGETS
G2M_CHECKPOINT
MYC_TARGETS_V1
MYC_TARGETS_V2
SPERMATOGENESIS
(D)
Deep SIG
Superficial SIG
Overall Survival
Percent survival
Months
(E)
Mixed stroma
Stem-like
Intestinal
Inflammatory
Gastric

◂**Fig. 2** Spatial differences in the tumor microenvironment between deep and superficial cell populations in diffuse-type gastric cancer. **A** t-SNE plots showing cell clustering and entropy scores for deep and superficial regions. Right-side bar plots display entropy levels and cluster distribution, highlighting deep-region enrichment of high-entropy cells. **B** GO enrichment networks for high-entropy clusters from deep (left) and superficial (right) regions. Deep clusters are enriched for apoptotic regulation and cytokine signaling, while superficial clusters are enriched for inflammatory responses and neutrophil degranulation. **C** Heatmaps of cancer hallmark pathway activity. Deep clusters show higher activity in angiogenesis, epithelial–mesenchymal transition (EMT), Hedgehog, and Notch signaling; superficial clusters are enriched for interferon and inflammatory pathways. **D** Kaplan–Meier survival curves from TCGA-STAD showing that high expression of deep-region (SIG47, left) and superficial-region (SIG131, right) gene signatures is associated with poor overall survival. **E** Box plots of SIG47 and SIG131 expression across five molecular subtypes in the Y497 cohort. SIG47 is enriched in gastric-type tumors, SIG131 in the inflammatory subtype; both are intermediately expressed in the stem-like subtype

Survival analysis

Gene signature prognostic relevance was evaluated using GEPIA2 (http://gepia2.cancer-pku.cn) [25], which accesses TCGA-STAD survival and expression data. For each signature, patients were stratified into high- and low-expression groups by median expression, and Kaplan–Meier survival curves were plotted. Significance was determined using the log-rank test with $p < 0.05$ considered significant.

Cell–cell communication analysis

To infer intercellular signaling patterns in the tumor microenvironment, we used the Cell Chat v1.5.0 R package [26]. Cell Chat was run on log-normalized expression matrices with precompiled human ligand–receptor interaction databases. Communication probabilities were calculated using the truncated mean method, and global signaling patterns were summarized via information flow scores. Signaling axes with total information flow > 0.1 were retained for visualization. Outgoing and incoming signaling roles were visualized using net Visual_circle and net Analysis_signaling Role functions, respectively.

Results

High-entropy cell populations are enriched in deep tumor regions

To explore the spatial organization of transcriptionally diverse cells in gastric cancer, we performed scRNA-seq on tumor tissues from five patients with diffuse-type gastric cancer. We compared cell states between the superficial and deep tumor regions, using entropy-based classification to identify high-entropy cell populations (Fig. 1A). These cells, which exhibit elevated transcriptional variability, were primarily localized to the deep tumor compartment in all five patients (Fig. 1B). Using the StemID algorithm, we confirmed that more than half of the high-entropy clusters were composed of cells from deep regions. These clusters were enriched for genes associated with the Naba core matrisome and VEGFA and VEGFR2 signaling pathways, with distinct gene sets depending on the cell type (Fig. 1C).

Tumor microenvironments differ between deep and superficial regions

We next characterized the tumor microenvironment in deep and superficial tumor regions by analyzing single-cell gene expression profiles and pathway enrichment signatures. Dimensionality reduction revealed marked compositional differences between the two regions (Fig. 2A). Specifically, the deep compartment showed a predominance of endothelial cells and fibroblasts with extracellular matrix (ECM)-remodeling features, consistent with a stromal-rich and vascularized niche. In contrast, the superficial compartment was enriched for immune lineages, including cytotoxic $CD8^+$ T cells and antigen-presenting dendritic cells, indicating a more immune-active microenvironment.

Functionally, high-entropy clusters within the deep region were enriched for gene ontology (GO) categories related to regulation of apoptosis, cytokine-mediated signaling, and immune cell activation, highlighting transcriptionally diverse stromal and vascular populations. Conversely, superficial clusters were enriched for pathways related to inflammatory responses, humoral immunity, and extracellular matrix organization (Fig. 2B). These spatially distinct enrichment patterns underscore that stromal remodeling and angiogenic signaling dominate in the deep tumor niche, while immune surveillance and inflammatory activity are more characteristic of the superficial region. Together, these findings provide mechanistic insights into how spatial variation in cell type composition and functional programs shape the tumor ecosystem.Cancer hallmark pathway analysis showed region-specific enrichment patterns in high-entropy clusters. Cells in the deep region exhibited higher activity in angiogenesis, epithelial-to-mesenchymal transition, coagulation, Notch signaling, myogenesis, apical junction formation, and Hedgehog signaling. Although some of these pathways were also enriched in superficial clusters, their activation was less pronounced (Fig. 2C).

To evaluate the clinical relevance of these gene expression patterns, we performed Kaplan–Meier survival analysis using TCGA-STAD data. Patients with high expression of a 47-gene signature derived from deep-region high-entropy cells (SIG47) showed significantly poorer survival compared

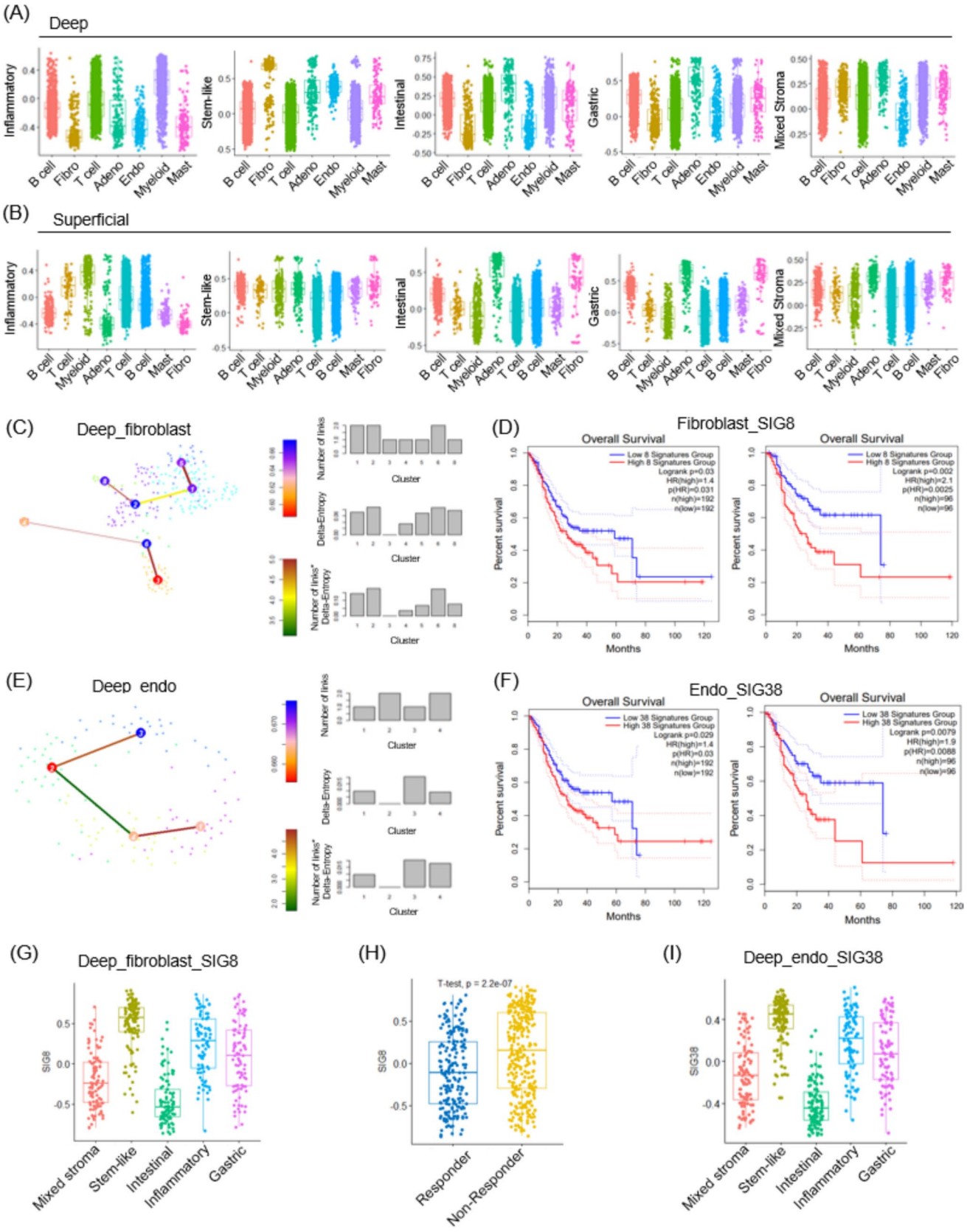
(A)
Deep
Inflammatory
Stem-like
Intestinal
Gastric
Mixed Stroma
B cell
Fibro
T cell
Adeno
Endo
Myeloid
Mast
(B)
Superficial
(C)
Deep_fibroblast
Number of links
Delta-Entropy
Number of links*Delta-Entropy
Cluster
(D)
Fibroblast_SIG8
Overall Survival
Low 8 Signatures Group
High 8 Signatures Group
Logrank p=0.03
HR(high)=1.4
p(HR)=0.031
n(high)=192
n(low)=192
Logrank p=0.002
HR(high)=2.1
p(HR)=0.0025
n(high)=96
n(low)=96
Percent survival
Months
(E)
Deep endo
(F)
Endo_SIG38
Low 38 Signatures Group
High 38 Signatures Group
Logrank p=0.029
HR(high)=1.4
p(HR)=0.03
n(high)=192
n(low)=192
Logrank p=0.0079
HR(high)=1.9
p(HR)=0.0088
n(high)=96
n(low)=96
(G)
Deep_fibroblast_SIG8
SIG8
Mixed stroma
Stem-like
Intestinal
Inflammatory
Gastric
(H)
T-test, p = 2.2e-07
Responder
Non-Responder
(I)
Deep_endo_SIG38
SIG38

◂**Fig. 3** Stem-like molecular signature enrichment and subtype-specific high-entropy gene sets. **A** Box plots showing enrichment scores for five gastric cancer molecular subtypes (stem-like, inflammatory, intestinal, gastric, mixed stroma) across deep-region single-cell types. Stem-like signatures are most enriched in fibroblasts and endothelial cells. **B** Two transcriptionally distinct T cell populations in the tumor microenvironment. Dimensionality reduction revealed the presence of two separate T cell clusters. One cluster corresponds to cytotoxic/TRM-like T cells, enriched for effector molecules (*CD8A, GZMB, PRF1, IFNG*) and indicative of robust cytolytic activity. The other cluster represents exhausted T cells, characterized by high expression of immune checkpoint and dysfunction-associated genes (*PDCD1, LAG3, HAVCR2, TOX*). Together, these populations highlight the coexistence of functionally divergent T cell states within gastric tumors, reflecting both active immune surveillance and chronic antigen-driven exhaustion. **C** t-SNE plot of deep-region fibroblasts. High-entropy clusters are highlighted with entropy and pseudotime scores, identifying a transcriptionally plastic fibroblast subpopulation. **D** Kaplan–Meier curves from TCGA-STAD for the fibroblast-derived signature (SIG8), showing significantly worse survival in high-expression groups. **E** t-SNE plot of deep endothelial cells with entropy and cluster distribution. **F** Kaplan–Meier curves for the endothelial-derived signature (SIG38), showing reduced survival in high-expression groups. **G–I** Box plots of SIG8 and SIG38 expression across molecular subtypes and ICB response groups in the Y497 cohort. Both signatures are most enriched in the stem-like subtype and are significantly upregulated in non-responders to ICB therapy

to those with low expression ($p = 0.0069$). Similarly, a 131-gene signature from superficial-region high-entropy clusters (SIG131) was also associated with worse survival ($p = 0.02$) (Fig. 2D). These gene signatures showed distinct subtype-specific expression patterns in the Y497 cohort, with SIG47 being highest in gastric-type tumors and SIG131 being most enriched in the inflammatory subtype. In the stem-like subtype, both gene sets exhibited intermediate expression levels (Fig. 2E).

Stem-like subtype signatures are enriched in deep fibroblasts and endothelial cells

We next examined the distribution of five established gastric cancer molecular subtype signatures at the single-cell level across tumor compartments. The stem-like signature was most prominently enriched in fibroblasts and endothelial cells within the deep region (Fig. 3A). Dimensionality reduction further revealed two transcriptionally distinct T cell clusters (Fig. 3B). One cluster was enriched for cytotoxic/TRM-like T cells, characterized by strong effector signatures including *CD8A, GZMB, PRF1*, and *IFNG*. In contrast, the second cluster represented exhausted T cells, defined by the expression of immune checkpoint and dysfunction-associated genes such as *PDCD1, LAG3, HAVCR2*, and *TOX*. These findings underscore the coexistence of functionally divergent T cell states within the tumor microenvironment.

We then focused on high-entropy subpopulations of fibroblasts and endothelial cells to identify subtype-specific gene signatures. Eight genes were identified in deep-region fibroblasts and 38 genes in endothelial cells (Fig. 3C, E). Kaplan–Meier survival analysis showed that high expression of the fibroblast signature (SIG8) and endothelial signature (SIG38) was significantly associated with poor overall survival in TCGA-STAD (Fig. 3D, F). These results were validated in the Y497 cohort, where both gene signatures were expressed at higher levels in tumors classified as stem-like (Fig. 3G). Notably, both SIG8 and SIG38 were significantly upregulated in patients who failed to respond to immune checkpoint blockade therapy, compared to responders (Fig. 3H, I).

Cell–cell signaling analysis reveals endothelial-derived interactions via the NAMPT-ITGA5-ITGB1 axis

To understand how endothelial and stromal cells contribute to the formation of the stem-like phenotype, we conducted cell–cell communication analysis using the Cell Chat framework. This analysis revealed that endothelial cells in the deep region were major sources of ligand expression, while fibroblasts, myeloid cells, and T cells received high levels of incoming signals (Fig. 4A).

Among several active signaling pathways, fibroblasts predominantly used the midkine-nucleolin (*MDK-NCL*) axis to interact with surrounding cells (Fig. 4B–E). In contrast, endothelial cells showed prominent signaling activity through the *NAMPT* pathway, using *ITGA5* and *ITGB1* as receptors (Fig. 4F–H).

To assess the clinical impact of this endothelial signaling axis, we evaluated the expression of *NAMPT, ITGA5*, and *ITGB1* in TCGA-STAD and found that their co-expression was associated with significantly worse survival outcomes (Fig. 4I). Furthermore, *ITGA5* expression was highest in the stem-like subtype and was significantly upregulated in non-responder patients within the Y497 cohort (Fig. 4J, K), suggesting its potential as a prognostic and predictive biomarker.

Discussion

Gastric cancer (GC) remains a significant global health burden, particularly in East Asia, and its stem-like molecular subtype represents the most aggressive clinical form, characterized by poor prognosis and resistance to conventional treatments, including immune checkpoint blockade (ICB) [27]. Although transcriptional subtypes of GC have been described, their spatial organization and the mechanisms driving stem-like evolution remain poorly defined.

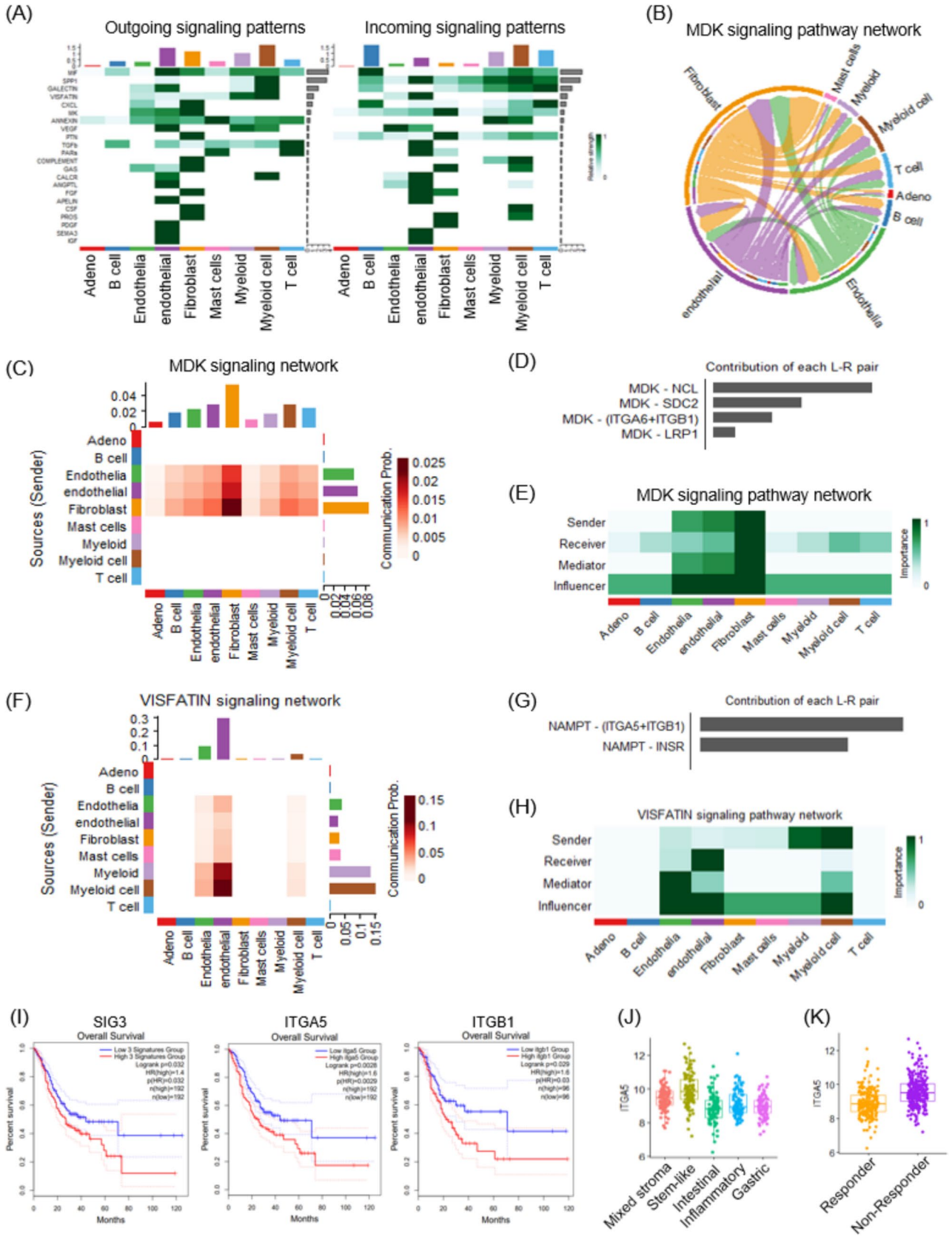
(A)
Outgoing signaling patterns
Incoming signaling patterns
Adeno
B cell
Endothelia
endothelial
Fibroblast
Mast cells
Myeloid
Myeloid cell
T cell
(B)
MDK signaling pathway network
(C)
MDK signaling network
Sources (Sender)
Communication Prob.
(D)
Contribution of each L-R pair
MDK - NCL
MDK - SDC2
MDK - (ITGA6+ITGB1)
MDK - LRP1
(E)
MDK signaling pathway network
Sender
Receiver
Mediator
Influencer
Importance
(F)
VISFATIN signaling network
(G)
Contribution of each L-R pair
NAMPT - (ITGA5+ITGB1)
NAMPT - INSR
(H)
VISFATIN signaling pathway network
(I)
SIG3
ITGA5
ITGB1
Overall Survival
Percent survival
Months
(J)
ITGA5
Mixed stroma
Stem-like
Intestinal
Inflammatory
Gastric
(K)
ITGA5
Responder
Non-Responder

◂**Fig. 4** Endothelial-derived *VISFATIN* signaling drives deep-region cell–cell communication. **A** Heatmaps of outgoing (left) and incoming (right) signaling strengths among major cell types in the deep TME, inferred by CellChat. Endothelial and fibroblast populations are prominent senders and receivers, respectively. **B** Circos plot of midkine (*MDK*) signaling showing directional interactions between fibroblasts, endothelial cells, and myeloid cells. **C** Heatmap of *MDK* pathway communication probabilities. **D** Bar plot of ligand–receptor (L–R) contributions to *MDK* signaling. The *MDK–NCL* axis is the top contributor. **E** Role classification of *MDK* signaling participants (sender, receiver, mediator, influencer), highlighting fibroblast dominance. **F** Heatmap of *VISFATIN* signaling probability, showing endothelial-to-stromal and immune interactions. **G** Bar plot identifying *NAMPT–ITGA5–ITGB1* as the primary L–R pair mediating *VISFATIN* signaling, followed by *NAMPT–INSR*. **H** Role classification of *VISFATIN* pathway participants, indicating that endothelial cells are major signal initiators. **I** Kaplan–Meier curves showing poor prognosis in TCGA-STAD patients with high expression of the *VISFATIN* signature (SIG3, left), *ITGA5* (middle), and *ITGB1* (right). **J**–**K** Box plots showing *ITGA5* expression across molecular subtypes and between ICB responders and non-responders in the Y497 cohort. ITGA5 is most enriched in the stem-like subtype and significantly upregulated in non-responders

Through single-cell transcriptomic analysis of diffuse-type GC, we identified high-entropy cell populations—defined by elevated transcriptional variability—predominantly localized in deep tumor regions. These cells were enriched for signaling pathways associated with extracellular matrix remodeling and angiogenesis, including *VEGFA–VEGFR2*, implicating the deep tumor microenvironment (TME) as a niche supporting cellular plasticity and malignancy [28]. Comparative analyses further confirmed that deep and superficial compartments are transcriptionally and functionally distinct, with deep regions exhibiting signatures of apoptosis regulation, cytokine signaling, and vascular remodeling, while superficial regions were enriched for inflammatory and humoral immune responses. These differences reflect distinct ecological pressures that likely shape tumor behavior and therapeutic response.

To assess the clinical relevance of these spatially localized transcriptional programs, we derived gene signatures from high-entropy clusters in both regions. The deep-region signature (SIG47) and the superficial-region signature (SIG131) were both significantly associated with poor overall survival in TCGA-STAD and showed distinct subtype associations: SIG47 was most enriched in gastric-type tumors, while SIG131 predominated in the inflammatory subtype [29].

Further analyses revealed that the stem-like subtype signature was predominantly localized to fibroblasts and endothelial cells in the deep tumor region. High-entropy subsets of these populations yielded two prognostically significant gene sets, SIG8 (fibroblast-derived) and SIG38 (endothelial-derived), respectively. These signatures were validated in the Y497 cohort, where they were significantly upregulated in non-responders to ICB therapy [28]. These findings suggest that both stromal and vascular components of the TME contribute to stem-like evolution and therapeutic resistance.

Beyond stromal and endothelial programs, our data also uncovered pronounced heterogeneity within the T cell compartment. Dimensionality reduction revealed two transcriptionally distinct T cell clusters: one corresponding to cytotoxic/TRM-like T cells (*CD8A, GZMB, PRF1, IFNG*) with robust effector potential, and the other representing exhausted T cells (*PDCD1, LAG3, HAVCR2, TOX*) marked by checkpoint expression and functional dysfunction. The coexistence of these divergent states suggests a spatially and functionally stratified immune landscape. In superficial regions, cytotoxic/TRM-like T cells were relatively more abundant, consistent with an immune-active niche, whereas exhausted T cells were preferentially localized to deep regions enriched for endothelial and ECM-remodeling fibroblast populations. This dichotomy highlights a critical interplay between immune surveillance and immune evasion, whereby chronic antigen exposure and stromal–vascular signaling in the deep tumor compartment drive T cell dysfunction. Importantly, these findings dovetail with our observation that deep-region endothelial cells engage in *NAMPT–ITGA5–ITGB1* signaling, a pathway linked to immunosuppression and checkpoint blockade resistance. Together, the integration of stromal, vascular, and immune programs underscores how the deep tumor niche orchestrates a coordinated strategy of immune escape, providing a mechanistic basis for therapeutic resistance in stem-like gastric cancer.

A key mechanistic insight from this study is the identification of *VISFATIN*-mediated signaling as a dominant mode of cell–cell communication within the deep tumor microenvironment. Using Cell Chat analysis, we found that endothelial cells serve as primary signal senders, with prominent activation of the *NAMPT–ITGA5–ITGB1* axis. Extracellular *NAMPT* (also known as *VISFATIN*) is thought to act in a cytokine-like fashion and has been suggested to interact with integrin α5β1 receptors, promoting tumor-supportive signaling between endothelial and immune cells [30]. Expression of this ligand–receptor triad was associated with poor survival in TCGA-STAD, and ITGA5 was particularly elevated in stem-like tumors and ICB-resistant cases [15].

Importantly, our findings expand the prevailing CAF-centric model of the stem-like TME by uncovering an alternative, endothelial-driven signaling route that independently contributes to disease progression and immunotherapy resistance. This represents the first single-cell-based evidence implicating endothelial-derived integrin signaling in spatially localized stem-like evolution, offering a paradigm shift in our understanding of TME dynamics in gastric cancer. While our analyses provide strong bioinformatics-based evidence for the *NAMPT–ITGA5–ITGB1* axis and its

association with immune evasion, we acknowledge that further in vitro and in vivo functional validation will be essential to establish direct mechanistic links and therapeutic relevance. Such experiments represent a critical next step and will be an important focus of future studies building upon the present work.

In conclusion, we present a spatially resolved and mechanistically detailed view of stem-like GC evolution. High-entropy endothelial cells in the deep tumor region promote tumor aggressiveness and immune evasion via VISFATIN-integrin signaling. These findings reveal functional heterogeneity within the stem-like subtype—distinguishing CAF-dominant from endothelium-dominant tumors—and propose a novel set of spatially defined biomarkers for patient stratification. From a precision medicine perspective, targeting endothelial signaling programs may offer new therapeutic avenues to overcome resistance in aggressive gastric cancer.

Conclusions

Our study identifies spatially distinct cellular programs underlying immune evasion in stem-like gastric cancer and reveals a novel VISFATIN–integrin signaling axis as a promising biomarker and therapeutic target for immunotherapy-resistant tumors.

Acknowledgements N/A

Author contributions JYS was responsible for the conceptualization, methodology development, data analysis, manuscript drafting, review, and editing, as well as the supervision of the study. JHC contributed to the review and editing of the manuscript. ETK provided funding acquisition, contributed to the interpretation of the results, and participated in the review and editing of the manuscript.

Funding This work was supported by the National Research Foundation of Korea (NRF), funded by the Ministry of Science and ICT (RS-2024–00352590) and the Ministry of Education (RS-2023–00270936), Republic of Korea. Additional support was provided by the Korea Health Technology R&D Project through the Korea Health Industry Development Institute (KHIDI), funded by the Ministry of Health & Welfare, Republic of Korea (RS-2022-KH129726, RS-2024–00438990).

Data availability No datasets were generated or analysed during the current study.

Declarations

Competing interest The authors declare no competing interests.

Consent for publication N/A.

Ethics Approval and Consent to Participate N/A

References

1. Mousavi SE et al (2025) Epidemiology and socioeconomic correlates of gastric cancer in Asia: results from the GLOBOCAN 2020 data and projections from 2020 to 2040. Sci Rep 15(1):6529
2. Sung JY, Cheong JH (2022) Prognosis-related gene signature is enriched in cancer-associated fibroblasts in the stem-like subtype of gastric cancer. Clin Transl Med 12(6):e930
3. Cheong JH et al (2018) Predictive test for chemotherapy response in resectable gastric cancer: a multi-cohort, retrospective analysis. Lancet Oncol 19(5):629–638
4. Sung JY, Cheong JH (2022) Intercellular communications and metabolic reprogramming as new predictive markers for immunotherapy responses in gastric cancer. Cancer Commun 42(6):572–575
5. Luo D et al (2025) Overcoming immunotherapy resistance in gastric cancer: insights into mechanisms and emerging strategies. Cell Death Dis 16(1):75
6. Yun H et al (2025) Role and value of the tumor microenvironment in the progression and treatment resistance of gastric cancer (Review). Oncol Rep 53(1):14
7. Sung JY, Cheong JH (2021) Alternative lengthening of telomeres is mechanistically linked to potential therapeutic vulnerability in the stem-like subtype of gastric cancer. Clin Transl Med 11(9):e561
8. Sung JY, Cheong JH (2023) Gene signature related to cancer stem cells and fibroblasts of stem-like gastric cancer predicts immunotherapy response. Clin Transl Med 13(8):e1347
9. Sung JY et al (2024) A subtype of cancer-associated fibroblast expressing syndecan-2 (SDC2) predicts survival and immune checkpoint inhibitor response in gastric cancer. Clin Transl Med 14(12):e70079
10. Sung JY, Cheong JH (2022) The matrisome is associated with metabolic reprograming in stem-like phenotypes of gastric cancer. Cancers 14(6):1438
11. Sung JY, Cheong JH (2021) Pan-cancer analysis reveals distinct metabolic reprogramming in different epithelial-mesenchymal transition activity states. Cancers (Basel). https://doi.org/10.3390/cancers13081778
12. Sung JY, Cheong JH (2022) New immunometabolic strategy based on cell type-specific metabolic reprogramming in the tumor immune microenvironment. Cells. https://doi.org/10.3390/cells11050768
13. Ozmen E, Demir TD, Ozcan G (2024) Cancer-associated fibroblasts: protagonists of the tumor microenvironment in gastric cancer. Front Mol Biosci 11:1340124
14. Liu J et al (2025) Hotspots and trends in gastric cancer stem cell research: a visualization and bibliometric analysis. Front Oncol 15:1523465

15. Peng Z et al (2023) Interactions between MFAP5 + fibroblasts and tumor-infiltrating myeloid cells shape the malignant microenvironment of colorectal cancer. J Transl Med 21(1):405
16. Ying L et al (2025) Predicting immunotherapy prognosis and targeted therapy sensitivity of colon cancer based on a CAF-related molecular signature. Sci Rep 15(1):6387
17. Jeong HY et al (2021) Spatially distinct reprogramming of the tumor microenvironment based on tumor invasion in diffuse-type gastric cancers. Clin Cancer Res 27(23):6529–6542
18. Grun D et al (2016) De novo prediction of stem cell identity using single-cell transcriptome data. Cell Stem Cell 19(2):266–277
19. Zhou Y et al (2019) Metascape provides a biologist-oriented resource for the analysis of systems-level datasets. Nat Commun 10(1):1523
20. Hanzelmann S, Castelo R, Guinney J (2013) GSVA: gene set variation analysis for microarray and RNA-seq data. BMC Bioinform 14:7
21. Lin X et al (2015) Molecular classification and prediction in gastric cancer. Comput Struct Biotechnol J 13:448–458
22. Kim M, Seo AN (2022) Molecular pathology of gastric cancer. J Gastric Cancer 22(4):273–305
23. Jang E et al (2023) Clinical molecular subtyping reveals intrinsic mesenchymal reprogramming in gastric cancer cells. Exp Mol Med 55(5):974–986
24. Ma Y et al (2024) Current development of molecular classifications of gastric cancer based on omics (Review). Int J Oncol. https://doi.org/10.3892/ijo.2024.5677
25. Tang Z et al (2019) GEPIA2: an enhanced web server for large-scale expression profiling and interactive analysis. Nucleic Acids Res 47(W1):W556–W560
26. Jin S et al (2021) Inference and analysis of cell-cell communication using cell chat. Nat Commun 12(1):1088
27. Jeon J, Cheong J-H (2019) Clinical implementation of precision medicine in gastric cancer. J Gastric Cancer 19(3):235–253
28. Li Y et al (2022) Single-cell landscape reveals active cell subtypes and their interaction in the tumor microenvironment of gastric cancer. Theranostics 12(8):3818–3833
29. Jeong YS et al (2023) Clinically conserved genomic subtypes of gastric adenocarcinoma. Mol Cancer 22(1):147
30. Gasparrini M, Audrito V (2022) NAMPT: a critical driver and therapeutic target for cancer. Int J Biochem Cell Biol 145:106189